Supporting Information

Structural Basis for Asymmetric Conductance of the Influenza M2 Proton Channel Investigated by Solid-State NMR Spectroscopy

Venkata S. Mandala, Shu Yu Liao, Byungsu Kwon and Mei Hong*

Department of Chemistry, Massachusetts Institute of Technology, Cambridge, MA 02139

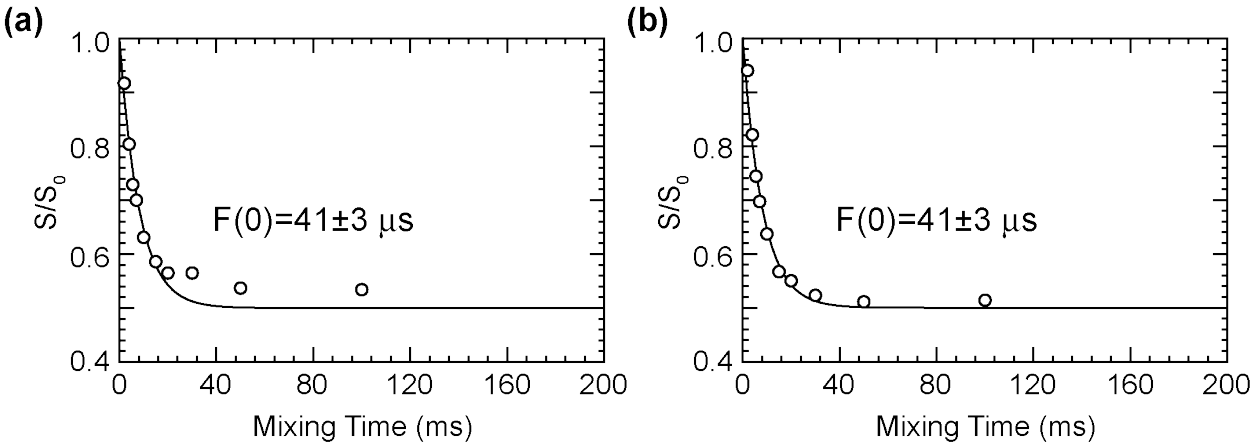

Figure S1. ^{19}F CODEX data of the model compound 5-^{19}F-Trp measured at 298 K on a 400 MHz spectrometer under (a) 10 kHz MAS. (b) 8 kHz MAS. Best-fit magnetization exchange curves used a ^{19}F-^{19}F nearest-neighbor distance of 4.62 Å. The best fit overlap integral, F(0), equals 41 μs for both datasets. The first z-filter time in the S_0 experiments was 1 ms in these experiments.

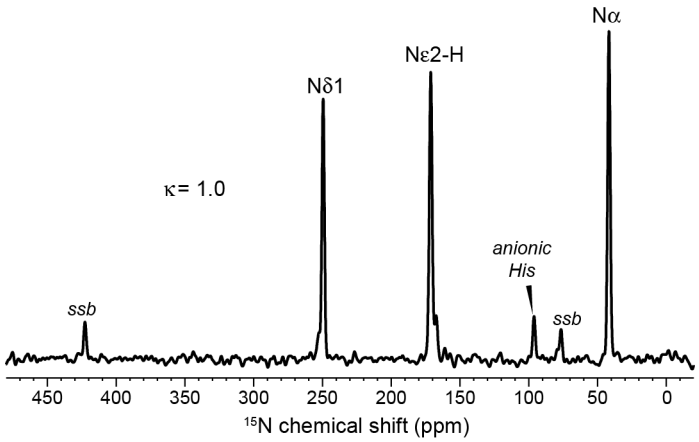

Figure S2. Representative ^{15}N MAS spectrum of U-^{13}C, ^{15}N-labeled histidine at pH 8.5. The ^{1}H-^{15}N CP contact time was 3 ms and the rf field strengths were 40 kHz for both ^{1}H and ^{15}N, with a moderate rf field ramp of 90-100% on the ^{15}N channel. The spectrum was measured at 293 K on a 400 MHz spectrometer under 7 kHz MAS. The unprotonated Nδ1 has a large CSA, giving rise to two sidebands (*ssb*). With these sideband intensities included, the integrated Nδ1 intensity is approximately the same as the Nε2-H peak intensity. The CP scaling factor, $\kappa = I_{NH}/I_N$, is 1.0 for this spectrum. The 98-ppm peak results from Nα of anionic His, which coexists with the zwitterionic form at this pH.

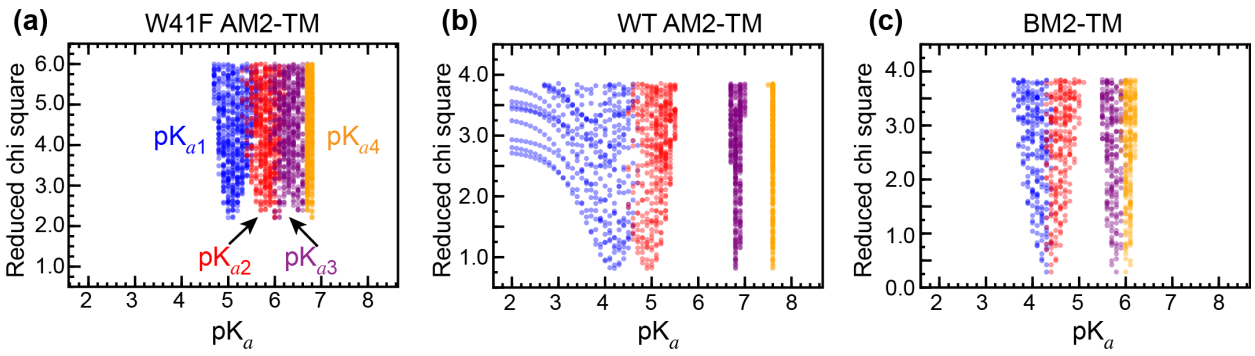

Figure S3. Statistical analysis of the distributions of the four H37 pK$_a$'s in (a) W41F AM2-TM, (b) WT AM2-TM, and (c) BM2-TM. The reduced chi-square values are calculated assuming 1 degree of freedom as described in the Experimental section.

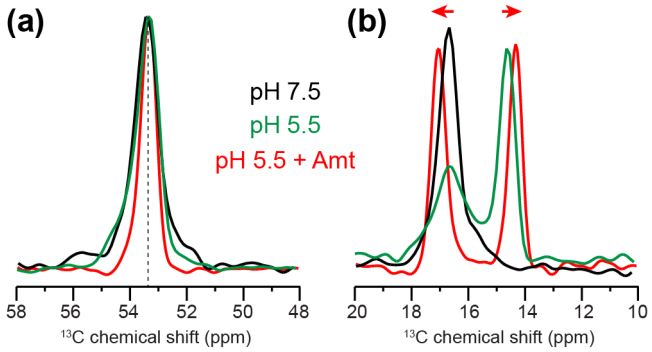

Figure S4. A30 cross sections extracted from 2D ^{13}C-^{13}C DARR spectra of W41F AM2-TM at pH 7.5 (black), pH 5.5 (green) and pH 5.5 with bound Amt (red). (a) The Cα cross section at 53.4 ppm, showing the same chemical shift for three samples. (b) Cβ cross sections. The Cβ peak at 16.7 ppm in the pH 7.5 and pH 5.5 samples moves downfield in the drug-bound sample, while the Cβ peak at 14.7 ppm in the pH 5.5 sample moves upfield in the drug-bound sample. Drug binding also narrows the linewidths. These observations indicate that all W41F AM2-TM channels contain bound drug.

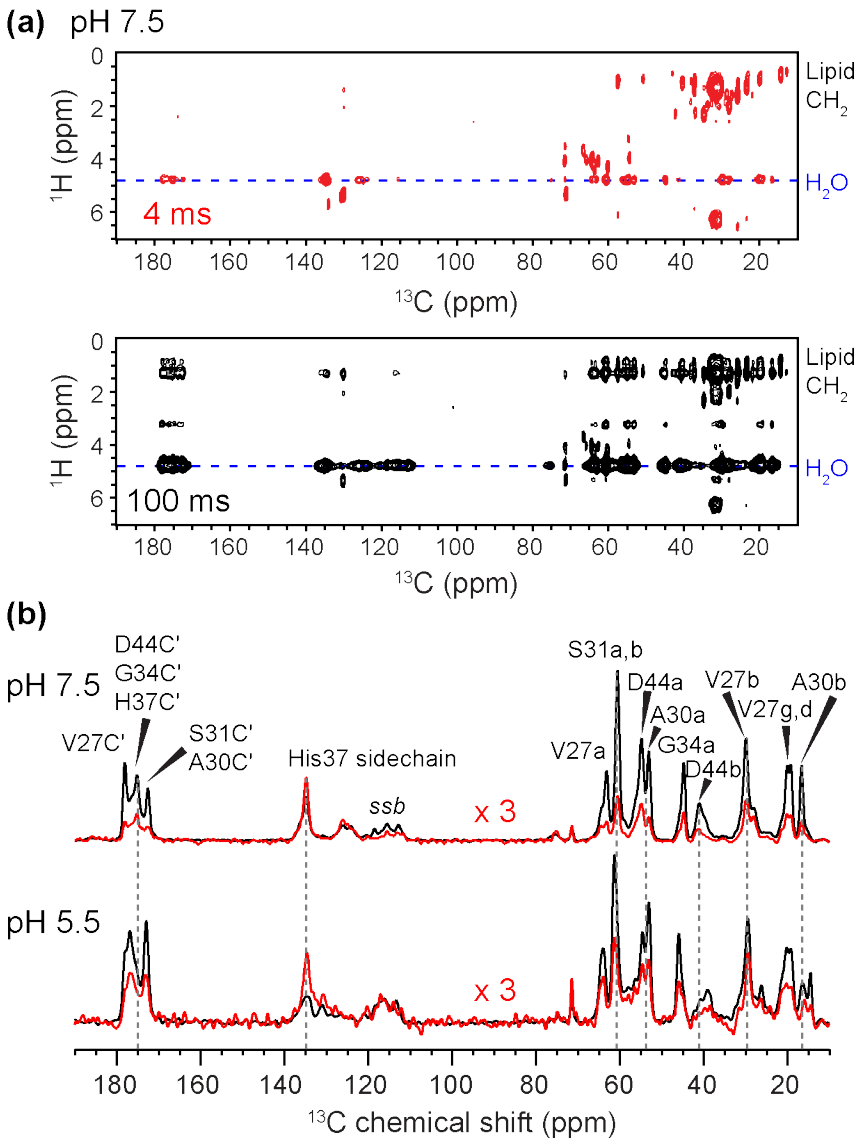

Figure S5. (a) 2D ^{1}H-^{13}C correlation spectra without ^{1}H homonuclear decoupling of W41F AM2-TM at pH 7.5. Spin diffusion mixing times were 4 ms for the S spectrum and 100 ms for the S_0 spectrum. The lack of ^{1}H-^{1}H homonuclear decoupling ensures that only the ^{1}H signals of mobile water and lipid are detected. (b) Water ^{1}H cross sections of the pH 7.5 and pH 5.5 samples at 4 ms (red) and 100 ms (black) mixing. The pH 5.5 sample shows higher intensities of the 4 ms spectrum relative to the pH 7.5 sample, indicating that the channel is better hydrated at low pH. The spectra were measured on an 800 MHz spectrometer at 293 K under 12 kHz MAS.

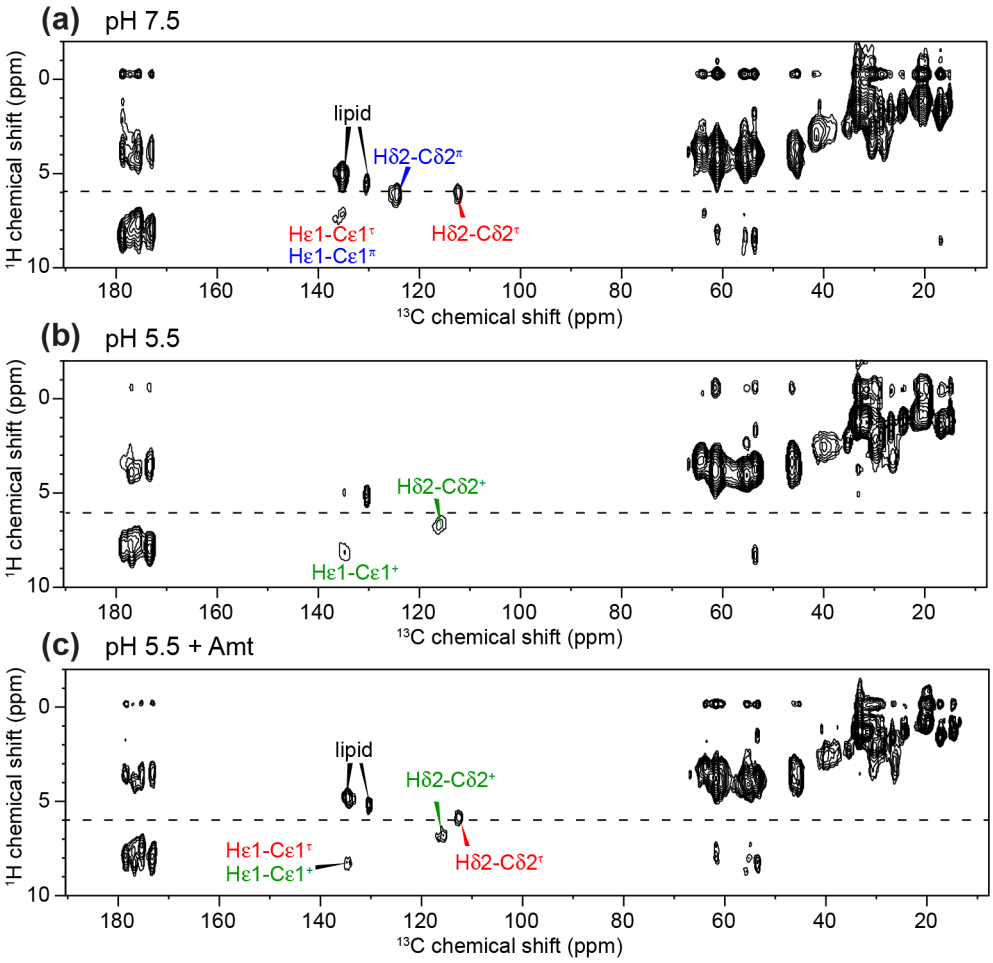

Figure S6. 2D ^{1}H-^{13}C correlation spectra with ^{1}H homonuclear decoupling of W41F AM2-TM. (a) pH 7.5; (b) pH 5.5; (c) pH 5.5 with bound Amt. His37 assignments are shown in red, blue and green for the τ tautomer, π tautomer, and cationic states, respectively. The spectra were measured at 263 K on an 800 MHz spectrometer. The ^{1}H-^{13}C LG-CP contact time was 300 μs and FSLG decoupling was applied during t_1.

Table S1. ^{13}C and ^{15}N chemical shifts (in ppm) of imidazole atoms of H37 in W41F AM2-TM. Asterisks denote peaks with partial overlap and thus larger chemical shift uncertainty.

H37 state	Cα	Cβ	Cγ	Cδ2	Cε1	Nε2	Nδ1
neutral, τ	55.8	30.7	136.1	112.1	135*	161	252*
neutral, π	55.8	27.8	126.0	124.2	135*	252*	170
cat1	59	29	128	114	135*	169*	169*
cat2	58	26	127	117	135*	175*	175*
cat3	56.5	25.9	131.1	115.7	134.1	176	181*
cat4	58.0	25.9	131.5	117.2	135*	175	181*

Table S2. Intensity ratios of H37 imidazole nitrogens in W41F AM2-TM. The scaling factor κ was measured before the experiment for each sample. The uncertainty in the scaling factor κ is estimated to be 0.05.

Sample pH	I_{NH}/I_N	κ	[His]/[$HisH^+$]
7.5	1.31±0.03	1.2	22.3±2.5
6.2	2.34±0.16	1.3	2.49±0.88
5.9	4.42±0.18	1.2	0.70±0.14
5.5	6.83±0.47	1.2	0.43±0.14
4.5	34.0±4.7	1.0	0.06±0.03

Table S3. Pearson product-moment correlation coefficient matrices for W41F AM2, WT AM2 and BM2.

	W41F AM2-TM				WT AM2-TM				BM2-TM			
	pK_{a1}	pK_{a2}	pK_{a3}	pK_{a4}	pK_{a1}	pK_{a2}	pK_{a3}	pK_{a4}	pK_{a1}	pK_{a2}	pK_{a3}	pK_{a4}
pK_{a1}	1.00	-0.36	-0.17	0.10	1.00	-0.59	0.03	-0.06	1.00	-0.76	0.35	-0.09
pK_{a2}	-0.36	1.00	-0.36	0.07	-0.59	1.00	-0.22	0.07	-0.76	1.00	-0.51	0.18
pK_{a3}	-0.17	-0.36	1.00	-0.41	-0.03	-0.22	1.00	-0.06	0.35	-0.51	1.00	-0.63
pK_{a4}	0.10	0.07	-0.41	1.00	-0.06	0.07	-0.06	1.00	-0.09	0.18	-0.63	1.00

Table S4. Approximate proton dissociation equilibrium constants K_a for WT and W41F M2 channels under different pH and drug binding conditions.

M2	High pH	Low pH	Low pH with drug
Wild type	$k_{off}^{'}/k_{on}$	$\left(k_{off}^{'}+k_{off}\right)/k_{on}$	k_{off}/ε
W41F	$\left(k_{off}^{'}+k_{off}^{W41F}\right)/k_{on}$	$\left(k_{off}^{'}+k_{off}^{W41F}\right)/\left(k_{on}+k_{on}^{'}\right)$	$K_a^{W41F,\,drug} \approx k_{off}^{W41F}/\left(k_{on}^{'}+\varepsilon\right)$